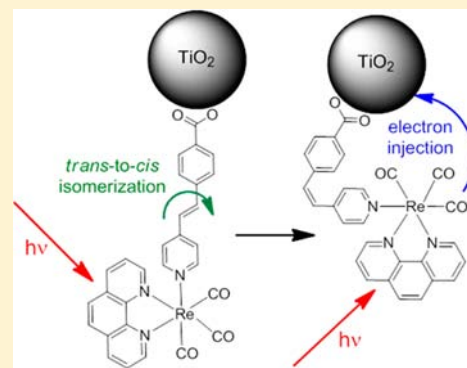


Solid State Molecular Device Based on a Rhenium(I) Polypyridyl Complex Immobilized on TiO₂ FilmsAntonio Otavio T. Patrocínio,[†] Karina P. M. Frin,[‡] and Neyde Y. Murakami Iha*[§][†]Instituto de Química, Universidade Federal de Uberlândia, Uberlândia 38400-902, Brazil[‡]Centro de Ciências Naturais e Humanas, Universidade Federal do ABC, Santo André 09210-170, Brazil[§]Laboratory of Photochemistry and Energy Conversion, Instituto de Química-USP, São Paulo 05508-900, Brazil

Supporting Information

ABSTRACT: The photochemical and photophysical behaviors of *fac*-[Re(CO)₃(phen)(*trans*-stpyCOOH)]⁺ (phen = 1,10-phenanthroline, *trans*-stpyCOOH = 4-[*trans*-(pyridin-4-yl-vinyl)]benzoic acid) in acetonitrile solution and adsorbed on a TiO₂ film have been investigated. The *trans*-to-*cis* photoisomerization at 404 nm irradiation of coordinated stpyCOOH occurs efficiently in fluid solution as shown by quantum yield determined spectrophotometrically ($\Phi_{UV-vis} = 0.37 \pm 0.04$) and, more accurately, by ¹H NMR ($\Phi_{NMR} = 0.48 \pm 0.04$), following the photoproduct signals in the distinct region of the reactant. For the first time, the *trans*-to-*cis* isomerization is also reported for the complex adsorbed on the TiO₂ surface ($\Phi_{UV-vis} = 0.23 \pm 0.03$). The photoproduct, *fac*-[Re(CO)₃(phen)(*cis*-stpyCOOH)]⁺, is emissive in acetonitrile ($\phi = 0.032$), but its radiative decay is highly quenched on the oxide surface by electron photoinjection into the semiconductor, leading to an increasing photocurrent as the *trans*-to-*cis* isomerization takes place. Therefore, the photoinduced *trans*-to-*cis* isomerization of coordinated ligand immobilized on TiO₂ films acts as a trigger for the electron injection process. This system exemplifies the use of photoinduced molecular motion to yield electrical current, which can be used as a “proof of concept” for molecular machines/devices.



INTRODUCTION

In recent years, significant research efforts have been devoted to the development of photoinduced molecular devices based on metal complexes.^{1–4} Potential applications include energy conversion,^{5,6} sensing,^{7–9} and molecular electronics.^{10–12} Rhenium(I) polypyridyl complexes have been extensively studied for application in molecular devices, due to their appropriate characteristics, such as chemical stability and easily tunable redox and spectroscopic properties by selecting the nature of ligands.^{13–18}

The development of molecular devices based on photoassisted *trans*-to-*cis* isomerization of coordinated stilbene-like ligands (L) is an interesting application of Re(I) polypyridyl complexes. Moreover, the [Re(CO)₃(NN)] chromophore sensitizes ligand isomerization to the visible, which allows the observation of the photoreaction in a spectral region where the ligand itself does not absorb.^{19,20} Theoretical^{21–23} and experimental^{24–26} studies have revealed the influence of polypyridyl ligands (NN) on the efficiency of this photoisomerization. Typically, the excitation of Re(I) complexes results in the population of a low energy ³MLCT_{Re→NN} state that sensitizes the low lying intraligand excited state ³IL_{trans-L} responsible for the isomerization.^{15,27} The photoproduct, the corresponding *cis*-isomer, usually exhibits a strong MLCT emission in fluid solution at room temperature, although the reverse *cis*-to-*trans* isomerization can be observed for a few complexes.²⁸

The immobilization of the active species on a suitable substrate, such as TiO₂ films, enhances the potential application of photoinduced *trans*-to-*cis* isomerization of coordinated stilbene-like ligands in Re(I) complexes. It will also be required that the molecular motion yields a signal, such as electrical current or luminescence, which can easily be processed in molecular devices, such as photoswitches and photosensors.

In this work, a novel complex *fac*-[Re(CO)₃(phen)(*trans*-stpyCOOH)]PF₆, phen = 1,10-phenanthroline, *trans*-stpyCOOH = 4-[*trans*-(pyridin-4-yl-vinyl)]benzoic acid, was synthesized and fully characterized in fluid media to be later immobilized in mesoporous nanocrystalline TiO₂ films (Scheme 1) with the aim of developing solid state molecular devices. The photochemical and photophysical behaviors of the adsorbed complex were investigated, and the sensitized film was employed in a photoelectrochemical cell as the photoanode. The results show that the photoisomerization acts as a trigger for electron injection, and this concept can be applied in solid state molecular devices.

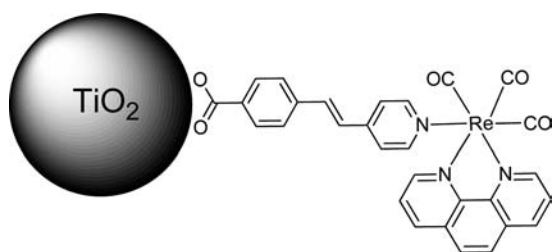
EXPERIMENTAL PROCEDURES

Materials. All chemicals were reagent grade, except HPLC solvents for photochemical and photophysical measurements. 4-Picoline, 4-carboxyaldehyde, acetic anhydride, trifluoromethanesulfonic acid

Received: December 28, 2012

Published: May 7, 2013

Scheme 1. *fac*-[Re(CO)₃(phen)(*trans*-stpyCOOH)]⁺ Adsorbed on a TiO₂ Nanoparticle



(CF₃SO₃H), potassium hydroxide, lithium iodide, titanium(IV) isopropoxide, all from Aldrich, and [ClRe(CO)₃] from Strem, were used as received. Potassium tris(oxalate)ferrate(III), employed as chemical actinometer, was synthesized and purified according to the literature procedure.²⁹

Syntheses. 4-[*trans*-(Pyridin-4-yl-vinyl)]benzoic Acid (*trans*-stpyCOOH). *trans*-stpyCOOH was prepared with slight modifications of procedure described for *trans*-4-styrylpyridine and its derivatives.³⁰ 4-Picoline (6.0 mL; 60 mmol) and 4-carboxybenzaldehyde (8.2 g; 45 mmol) were refluxed for 5 h in acetic anhydride (6.0 mL; 60 mmol), and the excess of 4-picoline was removed by distillation. The residual oil was dropped in water (0.5 L) to yield the crude product. Purification was achieved by recrystallization from 0.01 mol L⁻¹ KOH aqueous solution by slow addition of 1 mol L⁻¹ HCl. Yields 43%. Anal. Calc for C₁₄H₁₁NO₂·1/4H₂O: C, 73.19%; N, 6.10%; H, 5.05%. Found: C, 73.06%; N, 6.08%; H, 4.90%. ¹H NMR (as potassium salt; D₂O, δ/ppm): 8.48 (dd, 2H); 7.89 (dd, 2H); 7.70 (dd, 2H); 7.59, (dd, 2H); 7.53 (d, 1H); 7.28 (d, 1H).

fac-[Re(CO)₃(phen)(*trans*-stpyCOOH)]PF₆. The complex was synthesized according to the procedure previously described for *fac*-[Re(CO)₃(phen)(*trans*-stpy)]⁺ and other similar complexes.^{20,26,31} *fac*-[(CF₃SO₃)Re(CO)₃(phen)] (0.50 g; 0.80 mmol), previously synthesized,³¹ and *trans*-stpyCOOH (0.27 g; 1.2 mmol) were dissolved in 30 mL of methanol and heated to reflux for 9 h under argon atmosphere. After cooling to room temperature, the mixture was filtered to remove nonreacted *trans*-stpyCOOH. NH₄PF₆ was added to the filtrate to precipitate a yellow solid, which was separated by filtration. The solid was suspended in 15 mL of 0.1 mol L⁻¹ HCl and stirred for 1 h to remove the excess of NH₄PF₆. The product was separated by filtration and washed with water and ethyl ether. Yields 22%. Anal. Calc for ReC₂₉H₁₉N₃O₃PF₆: C, 42.44%; N, 5.12%; H, 2.33%. Found: C, 42.28%; N, 5.05%; H, 2.48%. ¹H NMR (CD₃CN, δ/ppm): 9.61 (dd, 2H); 8.84 (dd, 2H); 8.17 (m, 4H); 8.15 (dd, 2H); 7.91 (d, 2H); 7.58 (d, 2H); 7.39 (d, 1H); 7.28 (dd, 2H); 7.06 (d, 1H). Complete assignments of ¹H NMR peaks are provided in the Supporting Information (Table S1).

Preparation of Sensitized TiO₂ Films. TiO₂ nanoparticles were prepared by the sol-gel method as described previously.^{32,33} The films were deposited over transparent FTO substrates (fluorine doped tin oxide, TEC15-Pilkinton Co.) by painting. After drying at room temperature, the electrodes were sintered at 450 °C for 30 min. Sensitization of the TiO₂ surface was achieved by soaking sintered electrodes in acetonitrile solutions of *fac*-[Re(CO)₃(phen)(*trans*-stpyCOOH)]⁺ ranging from 1 × 10⁻⁵ to 1 × 10⁻⁴ mol L⁻¹.

Methods. Electronic absorption spectra were recorded on a Hewlett-Packard 8453 diode array spectrophotometer. ¹H NMR spectra were recorded on a DRX-500 (500 MHz) Bruker Avance spectrometer or on a Varian UNITY Inova (300 MHz) spectrometer using CD₃CN or D₂O as solvent. Residual CH₃CN or H₂O signals were used as an internal standard. Attenuated total reflectance infrared (ATR-FTIR) spectra were recorded in a Perkin-Elmer Spectrum Two spectrometer equipped with a PIKE ATR-MIRacle accessory. The measurements were recorded in a ZnSe crystal plate, using 32 scans at a resolution of 2 cm⁻¹. The spectra of adsorbed complex were obtained using a blank TiO₂ film as a background.

Photolyses of solutions at 313, 365, and 404 nm were carried out as previously reported,^{20,31} using an Oriel 200 W Hg(Xe) system by selecting the wavelength with appropriate interference filters. Samples were irradiated in a 1 cm quartz cuvette connected to a second quartz cuvette (0.1 cm) for direct absorption measurements. Light intensities were determined by tris(oxalate)ferrate(III) actinometry before and after each photolysis. Apparent *trans*-to-*cis* isomerization quantum yields were determined on the basis of absorbance decay of the *trans*-isomer, as previously described³¹ under conditions where the contribution of the *cis*-complex was minimized. For a more accurate determination, quantum yields at a given wavelength were plotted as a function of irradiation time and then extrapolated to zero time. True quantum yields were determined based on the areas of ¹H NMR signals for the *trans* and *cis* isomers along with absorption data, as described earlier.³⁴ *cis*-to-*trans* isomerization quantum yields at 254 nm for the photoproduct *fac*-[Re(CO)₃(phen)(*cis*-stpyCOOH)]⁺ were obtained using photolyzed solutions of the *trans*-isomer at the photostationary state as reported previously.^{19,35}

Photoisomerization experiments on TiO₂ films (1 cm² geometric area) over FTO were carried out in triplicate using a quartz cuvette under air with films parallel to the cuvette wall. In this setup, the electrode was held in a geometry that allowed the area irradiated to be analyzed spectrophotometrically. Photoisomerization quantum yields on adsorbed films were calculated by eq 1, in which *n_x* is the number of species that undergoes the photoreaction, *t_x* is the irradiated time (s), *I₀* is the light intensity at 404 nm, and *A_x* is the absorbance of the sensitized TiO₂ film at 404 nm (subtracting the absorbance of bare TiO₂).

$$\Phi = \frac{n_x}{I_0 t_x (1 - 10^{-A})} \quad (1)$$

n_x was calculated by using eq 2, in which $\epsilon(\lambda)$ is the molar absorptivity, $\Delta A(\lambda)$ is the absorbance variation at a selected wavelength, and *S* is the irradiated area in square centimeters. For accurate determination, absorption changes during photolyses were monitored at three different wavelengths and the conversion percentage was kept less than 10%.

$$n_x = \frac{(6.02 \times 10^{20}) \Delta A \times S}{\epsilon(\lambda)} \quad (2)$$

The molar absorptivity of adsorbed complexes was determined by eq 3, similar to the methodology described previously.^{36,37}

$$\epsilon(\lambda) = \frac{A}{1000 \Gamma_{\text{pro}}} \quad (3)$$

Surface coverage, Γ_{pro} , was determined spectrophotometrically by desorption of a nonirradiated film with 10⁻⁴ mol L⁻¹ NaOH in acetonitrile. ¹H NMR analysis of the photoproduct obtained by irradiation of the sensitized TiO₂ films was carried out in D₂O (10:1 (v/v) CD₃CN/40% KOD solution) with a series of desorbed films after photolyses.

Emission experiments were carried out in degassed acetonitrile solutions in a 1 cm quartz cuvette by using an ISS-PC1 photon counting spectrofluorometer, as previously reported.²⁶ Emission quantum yields were determined as described elsewhere³⁸ using the *fac*-[ClRe(CO)₃(phen)] complex ($\phi_{\text{em}} = 0.018$ in CH₃CN, 298 K) as standard. Time resolved emission data were acquired in an ISS-Chronos BH spectrometer coupled to a pulsed 378 nm diode laser (200 kHz; pulse width: 80–100 ps; peak power: 30–70 mW). Emission decays were monitored at various wavelengths, which were selected by using an ISS single concave holographic grating monochromator. The signals were detected at 90° with a PMC-100-4 Becker & Hickl photomultiplier interfaced to a computer. Reported lifetimes are the average of 1000 decay traces.

A photoelectrochemical cell, assembled in a homemade Teflon adapter, was irradiated by using an Oriel system comprised by a 400 W Xe lamp coupled to a 0.25 m Czerny-Turner monochromator as previously described.³⁹ Light intensity was measured with a thermopile

detector model 70261 connected to a power meter model 70260. Photocurrents were recorded with an Eco-Chemie PGSTAT-30 galvanostat/potentiostat. Sensitized TiO₂ films and a Pt-covered FTO were employed as photoanode and counter electrode, respectively, in a thin layer device.^{6,36,40–43} The photoanode was connected to the potentiostat counter electrode, and the cell counter electrode was connected to the working electrode short-circuited to the reference one. A 0.5 mol L⁻¹ LiI solution in acetonitrile was used as electrolyte.

RESULTS

The electronic spectrum of *fac*-[Re(CO)₃(phen)(*trans*-stpyCOOH)]PF₆ in acetonitrile (Figure 1a) is similar to that

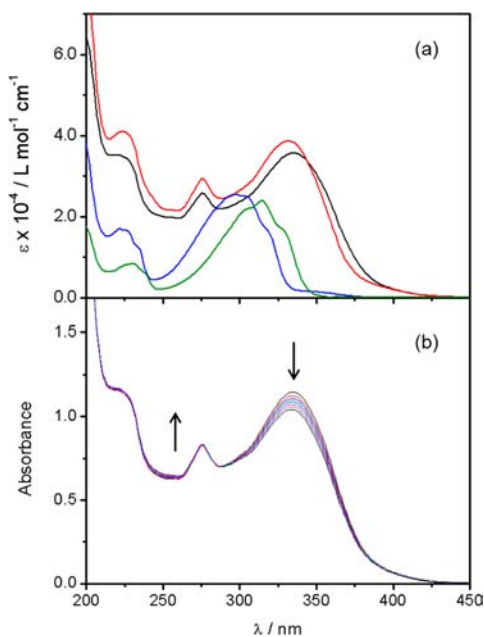


Figure 1. (a) Electronic spectra of *fac*-[Re(CO)₃(phen)(*trans*-L)]⁺, L = stpyCOOH (black line) or stpy (red line), of free *trans*-stpyCOOH (green line) and *trans*-stpy (blue line) in acetonitrile. (b) Spectral changes of *fac*-[Re(CO)₃(phen)(*trans*-stpyCOOH)]⁺ in acetonitrile under irradiation at 404 nm (3.2×10^{-4} mol L⁻¹; $\Delta t = 20$ s; $I_0 = 2.1 \times 10^{15}$ quanta s⁻¹).

of the parent complex *fac*-[Re(CO)₃(phen)(*trans*-stpy)]⁺, except for a small bathochromic shift of the low energy band, comparable to that observed for the free ligands, stpy and stpyCOOH. The broad, low energy band can be attributed to the overlapping of MLCT_{Re→phen} and IL($\pi\pi^*$)_{trans-L} transitions.

Irradiation of *fac*-[Re(CO)₃(phen)(*trans*-stpyCOOH)]⁺ in acetonitrile results in spectral changes ascribed to the *trans*-to-*cis* isomerization of the coordinated stpyCOOH ligand (Figure 1b). True quantum yields (Φ_{NMR}) determined by ¹H NMR, coupled with UV–vis, are shown in Table 1 and are similar, within experimental errors, to those found for *fac*-[Re(CO)₃(phen)(*trans*-stpy)]⁺.³⁴ The so-called true quantum yields for Re(I) polypyridyl complexes are higher than the apparent values determined only by absorption changes, $\Phi_{\text{UV-vis}}$ (shown in parentheses in Table 1), since the reactant and the photoproduct absorb in the same spectral region, not allowing an accurate quantum yield determination. Detailed discussion about the use of ¹H NMR spectroscopy for true quantum yield measurements can be found elsewhere.³⁴

The similarity of the isomerization quantum yields for *fac*-[Re(CO)₃(phen)(*trans*-stpyCOOH)]⁺ and values determined

Table 1. True *trans*-to-*cis* Photoisomerization Quantum Yields for *fac*-[Re(CO)₃(phen)(*trans*-L)]⁺ in CH₃CN at Different Irradiation Wavelengths^a

L	Φ (313 nm)	Φ (365 nm)	Φ (404 nm)
stpyCOOH	0.64 ± 0.02 (0.53 ± 0.05)	0.60 ± 0.03 (0.46 ± 0.07)	0.48 ± 0.04 (0.37 ± 0.04)
stpy ³⁴	0.59 ± 0.05 (0.35 ± 0.02)	0.60 ± 0.06 (0.31 ± 0.02)	0.43 ± 0.02 (0.29 ± 0.03)

^aApparent quantum yields are in parentheses.

for *fac*-[Re(CO)₃(phen)(*trans*-stpy)]⁺ allows us to conclude that the presence of the carboxylate group in the stilbene phenyl ring does not influence the efficiency of the isomerization process in solution. Higher quantum yields observed for both complexes at 313 or 365 nm irradiation are attributed to the contribution of the localized ¹IL_{trans-L} excited state, accessible only under UV irradiation, to the isomerization process.¹⁹

The photoproduct, *fac*-[Re(CO)₃(phen)(*cis*-stpyCOOH)]⁺, is emissive at room temperature in degassed acetonitrile. The emission spectrum is a broad, structureless band centered at 550 nm, which is similar to the spectrum of *fac*-[Re(CO)₃(phen)(*cis*-stpy)]⁺ (Figure 2). For both complexes,

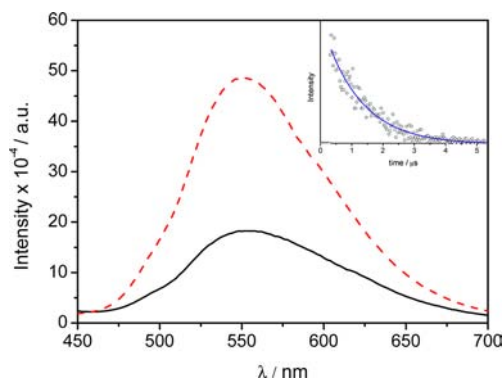


Figure 2. Emission spectra of *fac*-[Re(CO)₃(phen)(*cis*-L)]⁺, L = stpyCOOH (black line) and stpy (red dashed line) in argon-degassed acetonitrile ($\lambda_{\text{exc}} = 365$ nm). Inset: Emission decay traces at 550 nm (circles) of *fac*-[Re(CO)₃(phen)(*cis*-stpyCOOH)]⁺ in acetonitrile fitted to a monoexponential decay function (blue line); $\lambda_{\text{exc}} = 379$ nm.

emission lifetimes are approximately 1.2 μ s (Figure 2, inset), characteristic of ³MLCT emitters.²⁸ However, the emission quantum yield for the *cis*-stpyCOOH complex is 0.032; 40% lower than the value found for *fac*-[Re(CO)₃(phen)(*cis*-stpy)]⁺, showing that the presence of a carboxylate group increases the efficiencies of nonradiative deactivation pathways. Moreover, 254 nm irradiation of the photostationary state having up to 30:70 *trans*/*cis* ratio in solution leads to the *cis*-to-*trans* isomerization of *fac*-[Re(CO)₃(phen)(*cis*-stpyCOOH)]⁺ with a quantum yield of 0.14 ± 0.03 .

Continuous irradiation of acetonitrile solutions of the *trans*-isomer does not lead to 100% *cis*-to-*trans* conversion. This behavior has been observed for similar complexes,^{19,20,24,25,31,35,44,45} and it indicates a dynamic equilibrium between *trans*-to-*cis*/*cis*-to-*trans* isomerizations that does not result in net changes.²⁴

Adsorption of *fac*-[Re(CO)₃(phen)(*trans*-stpyCOOH)]⁺ on TiO₂ films deposited over FTO (fluorine doped tin oxide) electrodes results in pale yellow films. A maximum surface

coverage (Γ_{pro}) of 1.3×10^{-8} mol cm^{-2} was reached after 6–7 h of soaking at room temperature. The ATR-FTIR spectrum of the adsorbed complex (Figure 3a) is characterized by two broad

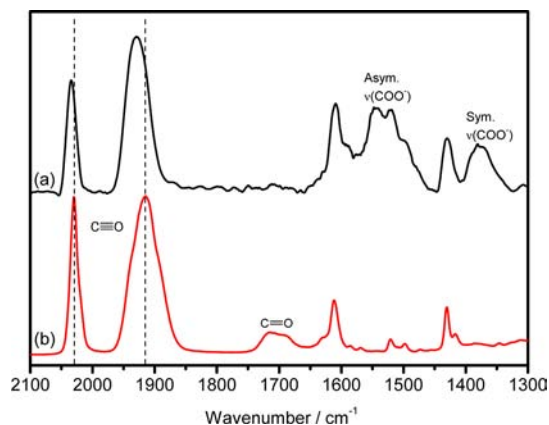


Figure 3. ATR-FTIR spectra of *fac*-[Re(CO)₃(phen)(*trans*-stpyCOOH)]⁺ (a) on TiO₂ and (b) in powder form.

bands at 1540 and 1380 cm^{-1} , attributed to asymmetric and symmetric carboxylate stretching modes. In comparison to the spectrum of the complex in the powder form (Figure 3b), the complete disappearance of the characteristic $\nu(\text{C}=\text{O})$ of the carboxylic acid group at 1715 cm^{-1} is observed. This behavior indicates that the adsorption of the complex on the oxide surface occurs by the binding of carboxylate groups to Ti^{4+} and confirms the absence of any physisorbed molecule on the surface. Similar data have been reported for other metal complexes having carboxylic acid as anchor group^{36,46–48} and are consistent with a monolayer adsorption model.

The ATR-FTIR spectrum of *fac*-[Re(CO)₃(phen)(*trans*-stpyCOOH)]⁺ on TiO₂ also exhibits two strong absorption bands at 2035 and 1930 cm^{-1} , typically observed in Re(I) tricarbonyl complexes in a *facial* geometry.^{31,49} These bands are blue-shifted in relation to those observed in the powder form, indicating that the adsorption on the oxide surface leads to a perturbation of $\nu(-\text{C}\equiv\text{O})$, probably due to local electric field interactions, as reported in the literature.⁵⁰

The derivatized films exhibit an increase in absorbance in comparison to the case of bare TiO₂ (Figure 4a), which is red-shifted compared to the spectrum of the complex in solution. The spectral shift can be related to the stabilization of the $\pi\pi^*$ intraligand transition in stpyCOOH by formation of the ester link between the carboxylate group and a Ti^{4+} ion at the surface and can be influenced by the change in the physical state of the complex.

Spectral changes of the complex adsorbed on TiO₂ films under 404 nm irradiation can be attributed to the *trans*-to-*cis* isomerization of coordinated stpyCOOH (Figure 4b). The formation of photoproduct, *fac*-[Re(CO)₃(phen)(*cis*-stpyCOOH)]⁺, was confirmed by ¹H NMR by desorbing the complex from the TiO₂ surface using an alkaline CD₃CN solution (Figure 5) (see the complete ¹H NMR spectral data in Table S1 of the Supporting Information).

Photoisomerization quantum yields for *fac*-[Re(CO)₃(phen)(*trans*-stpyCOOH)]⁺ adsorbed on TiO₂ films at different surface loadings are presented in Table 2. Detailed data as a function of irradiation time can be found in the Supporting Information (Table S2 and Figure S3). The photoreaction efficiency, 0.23 ± 0.03 ($\lambda_{\text{irr}} = 404$ nm), is independent on the

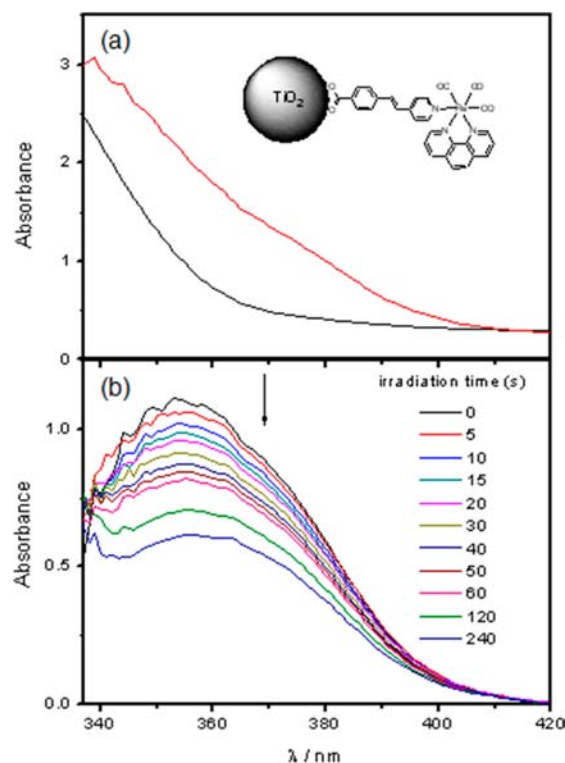


Figure 4. (a) Electronic absorption spectra of bare (—) and derivatized (red line) TiO₂ films on FTO; (b) Spectral changes of *fac*-[Re(CO)₃(phen)(*trans*-stpyCOOH)]⁺ on a TiO₂ film as a function of irradiation time (bare TiO₂ film as blank; $\Gamma = 1.06 \times 10^{-8}$ mol cm^{-2} ; $\lambda_{\text{irr}} = 404$ nm; $I_0 = 1.01 \times 10^{16}$ quanta s^{-1}).

surface coverage in the range 80–100%, in agreement with the monolayer absorption model. In fact, the large porous size of the TiO₂ film (2–50 nm) should not cause any steric hindrance during the molecular motion due to the isomerization process. Moreover, $\Phi_{\text{trans-cis}}$ determined by spectral changes is of the same magnitude found for other Re(I) polypyridyl complexes in solution¹³ and provides evidence that the *trans*-to-*cis* photoisomerization is the main deactivation process of *fac*-[Re(CO)₃(phen)(*trans*-stpyCOOH)]⁺ on TiO₂.

No luminescence is observed for the TiO₂ film loaded with ca. 70% *cis*-isomer complex, which allows us to conclude that the emission from the lowest lying ³MLCT_{Re→NN} excited state of the *cis*-isomer is highly quenched by electron injection, similarly to that reported for Ru(II) complexes.^{36,51} Electron injection by *fac*-[Re(CO)₃(phen)(*cis*-stpyCOOH)]⁺ was confirmed by irradiation at 400 nm in a thin layer photoelectrochemical cell using the derivatized TiO₂ film as a photoanode, a Pt-coated FTO as a counter electrode, and 0.5 mol L⁻¹ LiI in acetonitrile as an electrolyte. An instantaneous increase in the anodic current is observed as the light is turned on, due to electron injection of *fac*-[Re(CO)₃(phen)(*cis*-stpyCOOH)]⁺ into the TiO₂ conduction band (Figure 6). The current decays to zero when the light is turned off. The cycle can be repeated through multiple sequences; however, the maximum current reached falls as the number of cycles increases. Considering the first cycle, the *absorbed photon-to-current efficiency* (APCE) at 400 nm is approximately 4%.

Irradiation of a photoelectrochemical cell having only the *trans*-isomer derivatized TiO₂ film as a photoanode results in an initial photocurrent of ca. 0.08 μA , which is around 10% of the value observed for those starting with ~70% of *cis*-isomer under

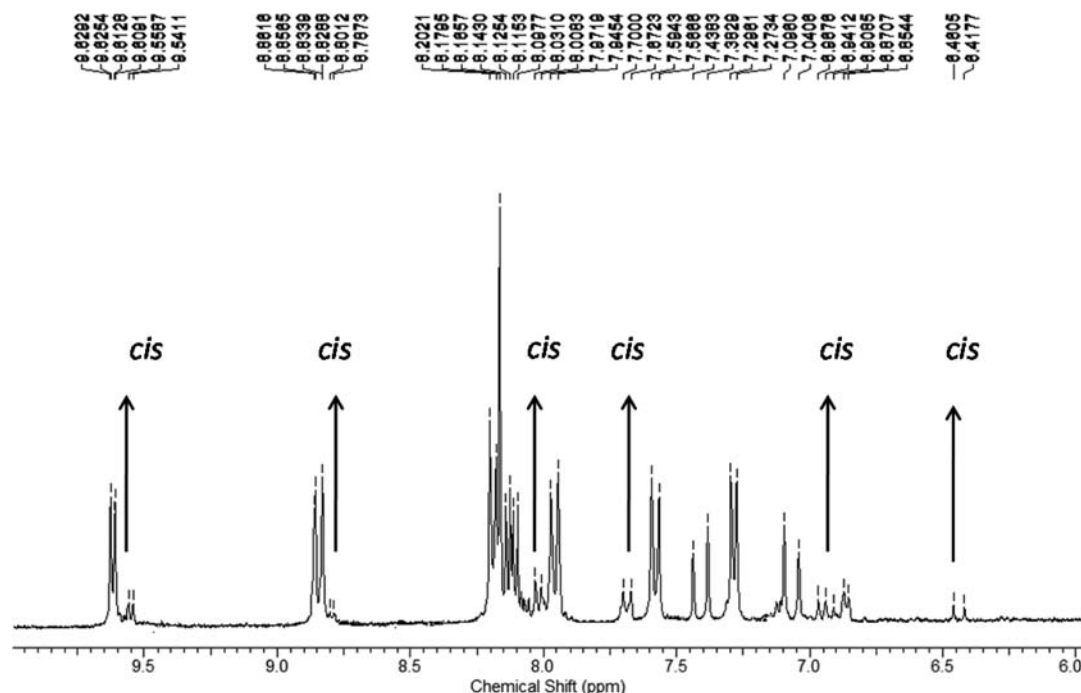


Figure 5. ^1H NMR spectrum of $\text{fac-}[\text{Re}(\text{CO})_3(\text{phen})(\text{stpyCOOH})]^+$ in alkaline CD_3CN desorbed from TiO_2 films after irradiation at 404 nm (300 MHz).

Table 2. *trans-to-cis* Photoisomerization Quantum Yields for $\text{fac-}[\text{Re}(\text{CO})_3(\text{phen})(\text{trans-stpyCOOH})]^+$ on TiO_2 at Different Surface Loadings Determined by Absorption Changes ($\lambda_{\text{irr}} = 404 \text{ nm}$)

Γ/Γ_0 (%)	$10^{16}I_0$ (quanta s^{-1})	$\Phi_{\text{UV-vis}}$
0.8	1.01	0.23 ± 0.02
0.9	0.99	0.24 ± 0.02
1.0	1.02	0.23 ± 0.01

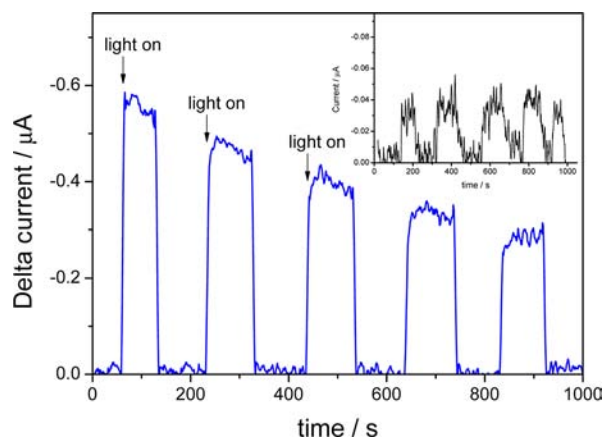


Figure 6. Electrical response of a photoelectrochemical cell employing a TiO_2 film derivatized by ca. 70% $\text{fac-}[\text{Re}(\text{CO})_3(\text{phen})(\text{cis-stpyCOOH})]^+$ on FTO as photoanode ($\lambda_{\text{irr}} = 400 \text{ nm}$). The response from bare TiO_2 under the same conditions (shown in the inset) was subtracted from the current measured.

the same experimental conditions. This considerable difference indicates that the electron injection on TiO_2 is the main deactivation pathway of the *cis*-isomer excited state on the surface, differently from the *trans*-isomer, in which the *trans-to-cis* isomerization is the main photoprocess. The observed

photocurrent increases as the photoisomerization takes place (Figure 7), due to formation of the photoproduct $\text{fac-}[\text{Re}(\text{CO})_3(\text{phen})(\text{cis-stpyCOOH})]^+$ on TiO_2 , yielding electrical current after a photoinduced molecular motion.

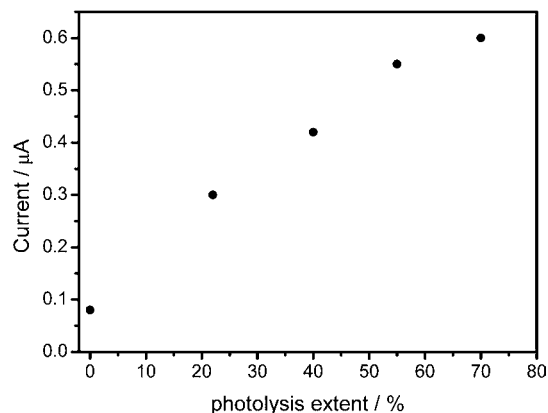


Figure 7. Photocurrent as a function of photolysis extent of $\text{fac-}[\text{Re}(\text{CO})_3(\text{phen})(\text{trans-stpyCOOH})]^+$ on TiO_2 ($\lambda_{\text{irr}} = 400 \text{ nm}$).

DISCUSSION

On the basis of the steady-state photoelectrochemical experiments, the excited state deactivation pathways for $\text{fac-}[\text{Re}(\text{CO})_3(\text{phen})(\text{stpyCOOH})]^+$ on a TiO_2 surface can be summarized as shown in Figure 8.

It is clear from the experimental data that (i) the occurrence of ligand-based *trans-to-cis* isomerization of $\text{fac-}[\text{Re}(\text{CO})_3(\text{phen})(\text{trans-stpyCOOH})]^+$ on a TiO_2 surface with a comparable quantum yield in relation to that observed in solution evidences that the photoisomerization is the main deactivation pathway of the *trans*-isomer in both media and (ii) the emissive decay observed for the *cis*-isomer in solution is

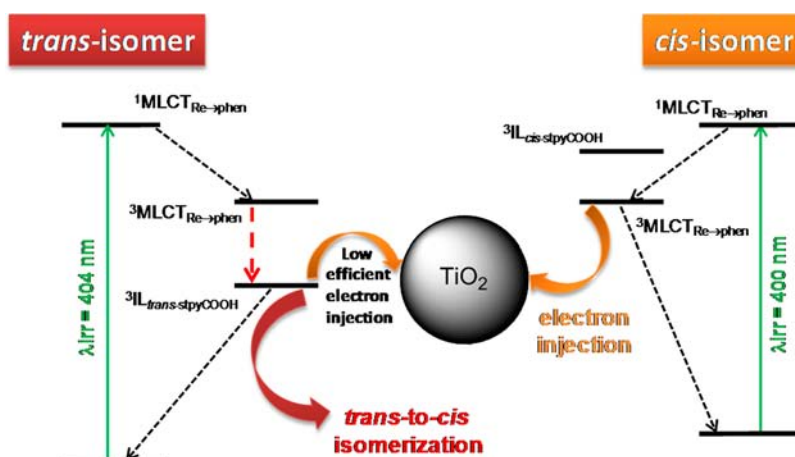


Figure 8. Simplified scheme for photoelectrochemical behavior of $fac-[Re(CO)_3(phen)(stpyCOOH)]^+$ on the TiO_2 surface.

completely quenched at the oxide surface due to electron injection into the TiO_2 conduction band. The differences between the photochemical and photophysical behaviors of the isomers on the oxide surface can be rationalized in terms of the nature of the low lying excited states in each isomer and their expected dynamics.

The photoinduced electron injection into the TiO_2 conduction band by adsorbed Re(I) or Ru(II) complexes usually has two components.⁵² The faster is attributed to singlet “hot” states and occurs on the femtosecond time scale. The slow component is derived from triplet states and occurs in the picosecond to nanosecond time domain, depending on the nature of the excited state, the bridging ligand, and the medium.^{53,54} Paoprasert et al. reported bridge dependent interfacial electron transfer kinetics in Re(I) polypyridyl complexes adsorbed on TiO_2 , showing that the contribution of 1MLCT injection decreases as the distance between the Re(I) center and TiO_2 surface increases.⁴⁷

It is also reported in the literature that the isomerization process of stilbene-like ligands coordinated to Re(I) polypyridyl complexes can be performed in a spectral region where the ligand itself does not absorb. The process occurs via a triplet mechanism for the *trans*-isomer, in which the population of the triplet ligand-base excited state, $^3IL_{trans-L}$, responsible for the isomerization, occurs via intramolecular sensitization from the $^3MLCT_{Re \rightarrow NN}$, as shown in Figure 8. Such a mechanism has been investigated theoretically^{21–23} and by time-resolved infrared spectroscopy (TRIR).^{27,55,56}

Irradiation of $fac-[Re(CO)_3(phen)(trans-stpyCOOH)]^+$ at 404 nm adsorbed on TiO_2 leads only to a population of $^1MLCT_{Re \rightarrow phen}$ without excitation of ligand-based transitions (Figure 1a). The observation of *trans-to-cis* isomerization in this wavelength excitation allows us to conclude that the population of the triplet ligand-base excited state, $^3IL_{trans-stpyCOOH}$, occurs efficiently.

Possible photoisomerization quenching pathways could involve direct ultrafast injection from 1MLCT or injection from triplet states. Considering that stpyCOOH is a relatively long bridging ligand, it is possible to understand the different photobehaviors of the two isomer complexes. Due to the heavy metal effect imparted by the Re(I) center, it is expected that the singlet state injection should have a minor contribution and the photoinjection should proceed via a triplet pathway. In fact, Lian and co-workers have shown that electron injection by

Re(I) complexes with longer alkyl bridges ($n > 1$) between the carboxylate group and the polypyridyl ligand occurs mostly by thermally relaxed 3MLCT excited states,^{53,57} as observed in $fac-[Re(CO)_3(phen)(cis-stpyCOOH)]^+$.

For Re(I) polypyridyl complexes with stilbene-like ligands, the lifetime of internal conversion from 3MLCT to $^3IL_{trans-L}$ is less than 10 ps in CH_3CN ,^{14,27} which is competitive with electron injection, according to the literature.^{53,57–59} This internal conversion occurs very efficiently on the basis of previous time-resolved absorption and infrared (TRIR) measurements for similar complexes, such as $fac-[Re(CO)_3(phen)(trans-bpe)]^+$ (ref 55) or $fac-[Re(CO)_3(phen)(trans-stpy)]^+$ (ref 27). Thus, it can be expected that electron injection from the 3MLCT excited state of $fac-[Re(CO)_3(phen)(trans-stpyCOOH)]^+$ on TiO_2 does not occur due to the ultrafast internal conversion to the lowest lying $^3IL_{trans-stpyCOOH}$ excited state. Once $^3IL_{trans-stpyCOOH}$ is populated, isomerization takes place in the nanosecond time domain, which is slow enough to be partially quenched by electron photoinjection. However, the isomerization process involves the formation of an intermediate triplet state 3p , in which the phenyl rings are perpendicular relative to each other.^{14,60} The interconversion to 3p occurs on the picosecond time domain, much faster than electron injection from $^3IL_{trans-stpyCOOH}$. The 90° rotation around the C=C bond in *trans-stpyCOOH* to yield the intermediate 3p excited state likely promotes the *trans-to-cis* isomerization.

Therefore, the observation of the isomerization as the major decay process in the *trans*-isomer is due to the nature of the lowest lying $^3IL_{trans-stpyCOOH}$ excited state and the very rapid internal conversion from $^3MLCT_{Re \rightarrow phen}$ to $^3IL_{trans-stpyCOOH}$. The strong electronic coupling between these triplet states leads to a fast and efficient population of the low energy $^3IL_{trans-stpyCOOH}$ responsible for the isomerization process.

In the *cis*-isomer, $fac-[Re(CO)_3(phen)(cis-stpyCOOH)]^+$, the lowest lying excited state is $^3MLCT_{Re \rightarrow phen}$ and electron injection occurs efficiently as shown by APCE experiments. Thus, the photoinduced *trans-to-cis* isomerization of the coordinated stpyCOOH ligand acts as a trigger for electron injection and is capable of yielding electrical current and being used as a signal in molecular devices.

CONCLUSIONS

This work showed, for the first time, photoinduced *trans*-to-*cis* isomerization of a stilbene-like ligand coordinated to a Re(I) polypyridyl complex on TiO₂. On the surface, *trans*-to-*cis* photoisomerization and electron injection are competitive pathways for excited state deactivation and can be controlled by the selection of ligands and/or by using semiconductors with different conduction band energies. For *fac*-[Re(CO)₃(phen)(*trans*-stpyCOOH)]⁺ on TiO₂, the photoisomerization process occurs with an apparent quantum yield of the same order as in solution ($\Phi = 0.23 \pm 0.03$; 404 nm irradiation) and can be considered the majority process. The photoproduct, *fac*-[Re(CO)₃(phen)(*cis*-stpyCOOH)]⁺, is emissive in solution, but when adsorbed on TiO₂, its luminescence is completely quenched by electron injection. This explains the rise in photocurrent as the concentration of the *cis*-isomer increases. The different behaviors of both isomers are rationalized in terms of the nature of the low lying excited state, ³IL_{*trans*-stpyCOOH} in the *trans*-isomer and ³MLCT_{Re→phen} in the *cis*-one. Thus, the electrical signal is controlled by a molecular motion, which opens the possibility of using the system in molecular devices.

ASSOCIATED CONTENT

Supporting Information

¹H NMR spectral data in CD₃CN for ligands and complexes, *trans*-to-*cis* photoisomerization quantum yields for *fac*-[Re(CO)₃(phen)(*trans*-stpyCOOH)]⁺ on TiO₂ ($\lambda_{\text{irr}} = 404$ nm) at different surface loadings as a function of irradiation time, and time-resolved emission spectra at different delay times of *fac*-[Re(CO)₃(phen)(*cis*-stpyCOOH)]⁺ in acetonitrile. This material is available free of charge via the Internet at <http://pubs.acs.org>.

AUTHOR INFORMATION

Corresponding Author

*Fax: +55(11)3815 5579. E-mail: neydeih@iq.usp.br.

Notes

The authors declare no competing financial interest.

ACKNOWLEDGMENTS

This work was supported by Fundação de Amparo à Pesquisa de São Paulo, FAPESP, Fundação de Amparo a Pesquisa de Minas Gerais, FAPEMIG, and Conselho Nacional de Desenvolvimento Científico e Tecnológico, CNPq. We would like to acknowledge Prof. Thomas J. Meyer for discussion and the manuscript reviewing of the first version.

REFERENCES

- (1) Saha, S.; Stoddart, J. F. *Chem. Soc. Rev.* **2007**, *36*, 77–92.
- (2) Balzani, V.; Bergamini, G.; Ceroni, P. *Coord. Chem. Rev.* **2008**, *252*, 2456–2469.
- (3) Morris, A. J.; Meyer, G. J.; Fujita, E. *Acc. Chem. Res.* **2009**, *42*, 1983–1994.
- (4) Pellegrin, Y.; Odobel, F. *Coord. Chem. Rev.* **2011**, *255*, 2578–2593.
- (5) Grätzel, M. *Acc. Chem. Res.* **2009**, *42*, 1788–1798.
- (6) Song, W. J.; Chen, Z. F.; Brennaman, M. K.; Concepcion, J. J.; Patrocínio, A. O. T.; Murakami Iha, N. Y.; Meyer, T. J. *Pure Appl. Chem.* **2011**, *83*, 749–768.
- (7) Kumar, A.; Sun, S. S.; Lees, A. J. Photophysics and photochemistry of organometallic rhenium diimine complexes. In

Topics in Organometallic Chemistry; Lees, A. J., Ed.; Springer: New York, 2010; Vol. 29, pp 1–35.

- (8) Itokazu, M. K.; Polo, A. S.; Murakami Iha, N. Y. *J. Photochem. Photobiol., A* **2003**, *160*, 27–32.
- (9) Wagenknecht, P. S.; Ford, P. C. *Coord. Chem. Rev.* **2011**, *255*, 591–616.
- (10) Hugel, T.; Holland, N. B.; Cattani, A.; Moroder, L.; Seitz, M.; Gaub, H. E. *Science* **2002**, *296*, 1103–1106.
- (11) Balzani, V.; Credi, A.; Venturi, M. *ChemPhysChem* **2008**, *9*, 202–220.
- (12) Santoni, M. P.; Hanan, G. S.; Hasenknopf, B.; Proust, A.; Nastasi, F.; Serroni, S.; Campagna, S. *Chem. Commun.* **2011**, *47*, 3586–3588.
- (13) Polo, A. S.; Itokazu, M. K.; Frin, K. M.; Patrocínio, A. O. T.; Murakami Iha, N. Y. *Coord. Chem. Rev.* **2006**, *250*, 1669–1680.
- (14) Vlcek, A., Jr. Ultrafast excited-state processes in Re(I) carbonyl-diimine complexes: From excitation to photochemistry. In *Topics in Organometallic Chemistry*; Lees, A. J., Ed.; Springer: New York, 2010; Vol. 29, pp 73–114.
- (15) Lin, J. L.; Chen, C. W.; Sun, S. S.; Lees, A. J. *Chem. Commun.* **2011**, *47*, 6030–6032.
- (16) Tapolsky, G.; Duesing, R.; Meyer, T. J. *Inorg. Chem.* **1990**, *29*, 2285–2297.
- (17) Gholamkhash, B.; Mametsuka, H.; Koike, K.; Tanabe, T.; Furue, M.; Ishitani, O. *Inorg. Chem.* **2005**, *44*, 2326–2336.
- (18) Christ, C. S.; Yu, J.; Zhao, X. H.; Palmore, G. T. R.; Wrighton, M. S. *Inorg. Chem.* **1992**, *31*, 4439–4440.
- (19) Patrocínio, A. O. T.; Murakami Iha, N. Y. *Inorg. Chem.* **2008**, *47*, 10851–10857.
- (20) Frin, K. M.; Murakami Iha, N. Y. *J. Braz. Chem. Soc.* **2006**, *17*, 1664–1671.
- (21) Gindensperger, E.; Koppel, H.; Daniel, C. *Chem. Commun.* **2010**, *46*, 8225–8227.
- (22) Bossert, J.; Daniel, C. *Chem.—Eur. J.* **2006**, *12*, 4835–4843.
- (23) Kayanuma, M.; Daniel, C.; Köppel, H.; Gindensperger, E. *Coord. Chem. Rev.* **2011**, *255*, 2693–2703.
- (24) Wenger, O. S.; Henling, L. M.; Day, M. W.; Winkler, J. R.; Gray, H. B. *Inorg. Chem.* **2004**, *43*, 2043–2048.
- (25) Yam, V. W. W.; Lan, V. C. Y.; Wu, L. X. *J. Chem. Soc., Dalton Trans.* **1998**, 1461–1468.
- (26) Polo, A. S.; Itokazu, M. K.; Murakami Iha, N. Y. *J. Photochem. Photobiol., A* **2006**, *181*, 73–78.
- (27) Busby, M.; Matousek, P.; Towrie, M.; Vlcek, A., Jr. *J. Phys. Chem. A* **2005**, *109*, 3000–3008.
- (28) Patrocínio, A. O. T.; Brennaman, M. K.; Meyer, T. J.; Murakami Iha, N. Y. *J. Phys. Chem. A* **2010**, *114*, 12129–12137.
- (29) Hatchard, C. G.; Parker, C. A. *Proc. R. Soc. London, A* **1956**, *235*, 518–536.
- (30) Chiang, M. C.; Hartung, W. H. *J. Org. Chem.* **1945**, *10*, 21–25.
- (31) Itokazu, M. K.; Polo, A. S.; de Faria, D. L. A.; Bignozzi, C. A.; Murakami Iha, N. Y. *Inorg. Chim. Acta* **2001**, *313*, 149–155.
- (32) Patrocínio, A. O. T.; Paterno, L. G.; Murakami Iha, N. Y. *J. Photochem. Photobiol., A* **2009**, *205*, 23–27.
- (33) Patrocínio, A. O. T.; Paniago, E. B.; Paniago, R. M.; Murakami Iha, N. Y. *Appl. Surf. Sci.* **2008**, *254*, 1874–1879.
- (34) Frin, K. P. M.; Itokazu, M. K.; Murakami Iha, N. Y. *Inorg. Chim. Acta* **2010**, *363*, 294–300.
- (35) Frin, K. P. M.; Zanoni, K. P. S.; Murakami Iha, N. Y. *Inorg. Chem. Commun.* **2012**, *20*, 105–107.
- (36) Brennaman, M. K.; Patrocínio, A. O. T.; Song, W.; Jurss, J. W.; Concepcion, J. J.; Hoertz, P. G.; Traub, M. C.; Murakami Iha, N. Y.; Meyer, T. J. *ChemSusChem* **2011**, *4*, 216–227.
- (37) Gallagher, L. A.; Serron, S. A.; Wen, X. G.; Hornstein, B. J.; Dattelbaum, D. M.; Schoonover, J. R.; Meyer, T. J. *Inorg. Chem.* **2005**, *44*, 2089–2097.
- (38) Worl, L. A.; Duesing, R.; Chen, P. Y.; Dellaciana, L.; Meyer, T. J. *J. Chem. Soc., Dalton Trans.* **1991**, 849–858.
- (39) Polo, A. S.; Murakami Iha, N. Y. *Sol. Energy Mater. Sol. Cells* **2006**, *90*, 1936–1944.

- (40) Patrocínio, A. O. T.; Paterno, L. G.; Murakami Iha, N. Y. *J. Phys. Chem. C* **2010**, *114*, 17954–17959.
- (41) Concepcion, J. J.; Jurss, J. W.; Brennaman, M. K.; Hoertz, P. G.; Patrocínio, A. O. T.; Murakami Iha, N. Y.; Templeton, J. L.; Meyer, T. *J. Acc. Chem. Res.* **2009**, *42*, 1954–1965.
- (42) Polo, A. S.; Itokazu, M. K.; Murakami Iha, N. Y. *Coord. Chem. Rev.* **2004**, *248*, 1343–1361.
- (43) Argazzi, R.; Murakami Iha, N. Y.; Zabri, H.; Odobel, F.; Bignozzi, C. A. *Coord. Chem. Rev.* **2004**, *248*, 1299–1316.
- (44) Frin, K. P. M.; Murakami Iha, N. Y. *Inorg. Chim. Acta* **2011**, *376*, 531–537.
- (45) Wrighton, M. S.; Morse, D. L.; Pdungsap, L. *J. Am. Chem. Soc.* **1975**, *97*, 2073–2079.
- (46) Kalyanasundaram, K.; Grätzel, M. *Coord. Chem. Rev.* **1998**, *177*, 347–414.
- (47) Paoprasert, P.; Laaser, J. E.; Xiong, W.; Franking, R. A.; Hamers, R. J.; Zanni, M. T.; Schmidt, J. R.; Gopalan, P. *J. Phys. Chem. C* **2010**, *114*, 9898–9907.
- (48) Nazeeruddin, M. K.; Humphry-Baker, R.; Liska, P.; Grätzel, M. *J. Phys. Chem. B* **2003**, *107*, 8981–8987.
- (49) Balk, R. W.; Stufkens, D. J.; Oskam, A. *J. Chem. Soc., Dalton Trans.* **1981**, 1124–1133.
- (50) Barbour, L. W.; Hegadorn, M.; Asbury, J. B. *J. Am. Chem. Soc.* **2007**, *129*, 15884–15894.
- (51) Bergeron, B. V.; Meyer, G. J. *J. Phys. Chem. B* **2003**, *107*, 245–254.
- (52) Thorsmolle, V. K.; Wenger, B.; Teuscher, J.; Bauer, C.; Moser, J.-E. *Chimia* **2007**, *61*, 631–634.
- (53) Anderson, N. A.; Lian, T. *Coord. Chem. Rev.* **2004**, *248*, 1231–1246.
- (54) Strouse, G. F.; Schoonover, J. R.; Duesing, R.; Meyer, T. *J. Inorg. Chem.* **1995**, *34*, 2725–2734.
- (55) Dattelbaum, D. M.; Itokazu, M. K.; Murakami Iha, N. Y.; Meyer, T. *J. Phys. Chem. A* **2003**, *107*, 4092–4095.
- (56) Butler, J. M.; George, M. W.; Schoonover, J. R.; Dattelbaum, D. M.; Meyer, T. *J. Coord. Chem. Rev.* **2007**, *251*, 492–514.
- (57) Asbury, J. B.; Anderson, N. A.; Hao, E. C.; Ai, X.; Lian, T. Q. *J. Phys. Chem. B* **2003**, *107*, 7376–7386.
- (58) Bignozzi, C. A.; Meyer, G. J. *ACS Symp. Ser.* **2003**, *844*, 154–170.
- (59) Meyer, T. J.; Meyer, G. J.; Pfennig, B. W.; Schoonover, J. R.; Timpson, C. J.; Wall, J. F.; Kobusch, C.; Chen, X. H.; Peek, B. M.; Wall, C. G.; Ou, W.; Erickson, B. W.; Bignozzi, C. A. *Inorg. Chem.* **1994**, *33*, 3952–3964.
- (60) Saltiel, J.; Marinari, A.; Chang, D. W. L.; Mitchener, J. C.; Megarity, E. D. *J. Am. Chem. Soc.* **1979**, *101*, 2982–2996.